Water Practice & Technology Vol 15 No 4
doi: 10.2166/wpt.2020.086

Nitrate removal in potable groundwater by nano zerovalent iron under oxic conditions

Jayanga Kodikara, Buddhika Gunawardana*, Mahesh Jayaweera, Madhusha Sudasinghe and Jagath Manatunge

Department of Civil Engineering, University of Moratuwa, Moratuwa, Sri Lanka

*Corresponding author. E-mail: buddhikag@uom.lk

Abstract

Groundwater pollution by nitrate contamination has become a significant issue in some areas of Sri Lanka, giving rise to health concerns and a dearth in good quality potable water. In this study, the effectiveness of nano zerovalent iron (nZVI) for the removal of nitrate in potable groundwater under oxic conditions was investigated to meet the drinking water quality standards stipulated by World Health Organization (WHO) and Sri Lanka Standards Institution (SLSI) (nitrate level <50 mg/L). Under oxic conditions, the nZVI was synthesized and batch experiments were conducted using an artificial nitrate (150 mg/L) contaminated water sample. Our results corroborated that with an optimum nZVI dose of 1 g/L and optimum contact time of 30 minutes, 80% nitrate removal could be achieved and the remaining nitrate level was ≈ 30 mg/L as nitrate (<50 mg/L), which was equivalent to ≈ 7 mg/L as nitrate–N (≈21% of the total–N). Ammonium ions were the main product of nitrate reduction by nZVI and at 30 minutes contact time, ≈ 20 mg/L of ammonium as ammonium–N was detected (≈ 59% of the total–N). Ammonia stripping took place under the basic solution pH (pH > 9.5). At 30 minutes of contact time, ≈7 mg/L of ammonia as ammonia–N was accounted for ammonia stripping, which is 20% of the total–N. Ammonia stripping resulted in a decrease in nitrogen-containing species in the aqueous phase. The spent nZVI particles were recovered (99.9%) from the treated water using an external magnetic field. In conclusion, nZVI particles synthesized under oxic conditions are viable to successfully treat the nitrate-contaminated groundwater under aerobic conditions to reduce the nitrate levels to meet the WHO/SLSI drinking water quality standards.

Key words: ammonia, groundwater contamination, iron, nanoparticles, nitrate removal, nZVI

Highlights

- nZVI was synthesized under oxic conditions.
- Nitrate (150 mg/L) in ground water was removed to levels less than 50 mg/L (WHO guideline for drinking water quality).
- Nitrate was removed (80% removal at 30 minutes) by reduction to ammonium followed by ammonia stripping.
- Spent nZVI was completely removed from water using a magnetic field.
- This nZVI could be used in a domestic water filter for nitrate removal.

Water Practice & Technology Vol 15 No 4
doi: 10.2166/wpt.2020.086

Graphical Abstract

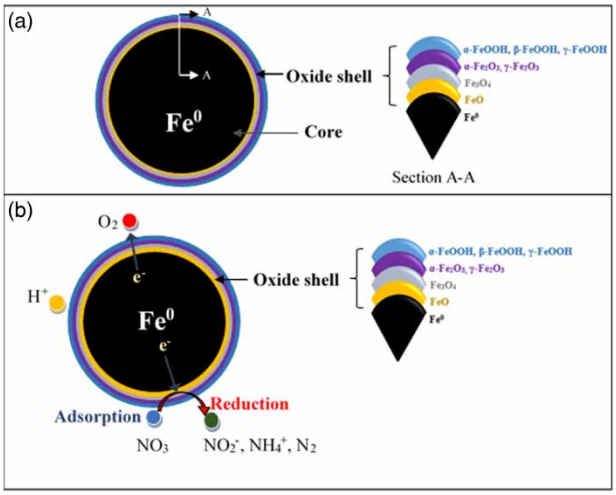

INTRODUCTION

Nitrate has emerged as one of the foremost alarming and widespread contaminants of groundwater and surface water resources in many parts of the world (Shukla & Saxena 2018). Nitrate contamination has been reported in groundwater sources in Sri Lanka in the range of 10–366 mg/L, especially in areas such as Anuradhapura, Jaffna, Kilinochchi, Mannar, Vavuniya, and Puttalam (Herath 2018). The nitrate levels detected in groundwater in 13 out of 25 districts in Sri Lanka have been over 50 mg/L (Herath 2018). While some areas have been identified to have extremely high nitrate levels (366 mg/L as stated above), about 95% of the nitrate concentrations reported in groundwater sources of these 13 districts in Sri Lanka have been between 10 and 150 mg/L (Gunatilake & Iwao 2010; Gunatilake 2016; Nijamir & Kaleel 2017; Herath 2018).

The possible underlying factors for the nitrate contamination of groundwater sources in many areas are identified as agricultural runoff, inappropriately located septic and soakage systems, leaching of nitrogenous fertilizers, and unplanned wastewater discharges from industrial sectors (Liyanage *et al.* 2000; Vaheesar 2002; Bawatharani *et al.* 2004; Mikunthan *et al.* 2013; Gunatilake 2016; Khalil *et al.* 2016; Wijeyaratne & Subanky 2017).

The presence of elevated levels of nitrate in potable groundwater poses drastic negative impacts on human health. Specifically, infants are the most vulnerable group as the consumption of nitrate-contaminated water can inflict methemoglobinemia (blue baby syndrome). In the meantime, drinking water contaminated with high levels of nitrate propels several other health issues such as immunological abnormalities, thyroid disorders, cancers, and liver damages (Bhatnagar *et al.* 2010; Khalil *et al.* 2016). In response to the potential health hazards for human beings from exposure to high nitrate levels in drinking water, both the World Health Organization (WHO 2017) and Sri Lanka Standards Institution (SLS 2013) have stipulated a concentration of 50 mg/L of nitrate (as NO_3^-) in drinking water for short and long term exposure conditions of infants and adults.

The removal of excessive nitrate levels present in potable groundwater is an essential need to provide safe drinking water for the consumers. Chemical and biological methods have been used to reduce nitrate concentration in potable water with varying degrees of efficiencies. Some of the methods adopted for nitrate removal in water include selective ion exchange (Samatya *et al.* 2006), reverse osmosis (Schoeman & Steyn 2003), electrodialysis (Schoeman 2009), chemical reduction using granular zerovalent iron (Rocca *et al.* 2007), and biological denitrification (Mohamed & Lee 1988). Also, different adsorbents such as chitosan (Chatterjee & Woo 2009), carbon cloth (Afkhami

Water Practice & Technology Vol 15 No 4
doi: 10.2166/wpt.2020.086

et al. 2007), carbon nanotubes (Khani & Mirzaei 2008), and modified zeolite (Arora *et al.* 2010) have been used for removing nitrate from water. Further, Eljamal & co-workers (2008) reported a significant reduction in nitrate levels with the application of the bioremediation process with sawdust as a matrix. However, these methods have several disadvantages and limitations. In general, ion exchange, reverse osmosis, and electrodialysis are expensive treatment processes and dispose of a concentrated waste containing nitrate, which is produced during the treatment, to the environment (Rocca *et al.* 2007). Ion exchange is not suitable for water with high total dissolved solids (Schoeman 2009). Reverse osmosis requires high energy for operation (Archna *et al.* 2012). Drawbacks of the electrodialysis process include high system complexity during operation and energy demand (Jensen *et al.* 2012). Disadvantages of the biological denitrification process include the accumulation of microbial degradation products in treated water, leading to bacteriological contamination of potable water and associated health risks (Ratnayake *et al.* 2017), and high capital and monitoring costs (Jensen *et al.* 2012). Adsorption using various adsorbents may not be effective and applicable for *in-situ* treatment of potable water because of the possible interferences from the impurities that are simultaneously present with nitrate in aquifers (Rocca *et al.* 2007).

Among various technologies proposed to remove nitrate in potable water, nano zerovalent iron (nZVI) has been reported as an effective reductant (Ratnayake *et al.* 2017). In comparison to other technologies, the application of nZVI is effective and superior in nitrate reduction from nitrate-contaminated groundwater because of its effective surface to volume ratio, high electron-donating potency, nano-scale, unique atomic properties, magnetic properties, and abundance (Hwang *et al.* 2011; Ryu *et al.* 2011; Ratnayake *et al.* 2017; Elshafai *et al.* 2018). Also, the use of nZVI does not lead to the generation and discharge of concentrated waste during the treatment process. Although zerovalent iron (ZVI) is a reactive metal with a relatively high standard redox potential (E° of −0.44 V, Liu & Wang 2019), in comparison to granular ZVI, nZVI comprises larger specific surface area and higher surface reactivity, thus would be more efficient in treating contaminants in groundwater (Peng *et al.* 2015).

nZVI has been employed in many environmental remediation applications. Eljamal & co-workers (2018, 2019) reported high phosphorous removal (30 mg/g) from aqueous solutions using nZVI. Further, nZVI has been used for Fenton oxidation and complete removal of phenol from aqueous solution has been reported (Babuponnusami & Muthukumar 2012). Besides, nZVI has been applied for the removal of azo dyes (Fan *et al.* 2009), pesticides such as heptachlor, lindane, hexachlorobenzene (Šimkovič *et al.* 2015), halogenated organic compounds such as dichlorophenyltrichloroethane (Poursaberi *et al.* 2012), trichloroethylene (Kim *et al.* 2010), pharmaceuticals such as metronidazole (Fang *et al.* 2011), amoxicillin, and ampicillin (Ghauch *et al.* 2009), and inorganic contaminants such as Pb^{2+} (Esfahani *et al.* 2014), and Ni^{2+} (Nazli 2008). Further, Diao & Yao (2009) reported complete inactivation of gram-positive *Bacillus subtilis var. niger* and gram-negative *Pseudomonas fluorescens* bacteria with the application of nZVI.

In general, nZVI comprises a core structure predominantly with Fe^0 and a shell structure made of iron oxides, which is formed via the oxidation of Fe^0 in the core by water and oxygen during the synthesis process (Figure 1(a)) (Mu *et al.* 2017). Initially, Fe^{2+} is formed as shown in Equations (1) and (2) to form the shell, where Equation (1) is thermodynamically favored. Subsequently, oxidation can occur to produce Fe^{3+} within the shell (Equations (3) and (4)). The Fe^{3+} so formed in the shell could react with OH^- to produce $Fe(OH)_3$ (Equation (5)), and it may dehydrate to FeOOH (Equation (6)). The nZVI exposed to further oxic conditions could grow into a distinct core-shell structure through continuous Fe^0 (in the core) oxidation process, resulting in the formation of oxide phases in the sequence of wüstite (FeO), magnetite (Fe_3O_4), maghemite (γ-Fe_2O_3), and hematite (α-Fe_2O_3) (Equations (7)–(9)) in its shell structure (Figure 1(a)) (Mu *et al.* 2017).

The formation of a thick layer of iron oxides (maghemite (γ-Fe_2O_3) or lepidocrocite (γ-FeOOH)) in the shell structure acts as a physical barrier, deteriorating the performance of nZVI (Liu & Wang

Water Practice & Technology Vol 15 No 4
doi: 10.2166/wpt.2020.086

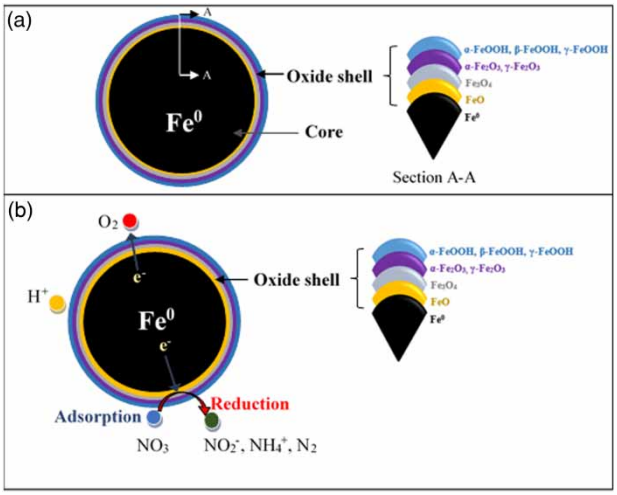

Figure 1 | (a) Schematic diagram of the core-shell structure of nZVI; (b) Graphical representation of adsorption and reduction mechanisms of nitrate by nZVI under oxic conditions.

2019). Interestingly, Huang & Zhang (2005) report that when the dissolved oxygen (DO) levels deplete under environmental conditions favorable for Fe(II), the adsorption of Fe(II) on to γ-FeOOH (e.g. ambient temperature and pH > 7.3) takes place, transforming γ-FeOOH to Fe_3O_4. It has been noted that Fe_3O_4 has the highest conductivity of all iron oxides (Cornell & Schwertmann 2003), thus would not hinder the electron transfer from the nZVI core to nitrate ions (Liu & Wang 2019). The Fe^0 tends to further oxidize under aerobic conditions where dissolved oxygen (DO) and H^+ (in the aqueous medium) act as the electron acceptors (Equation (10)) (Ghosh *et al.* 2017). The primary products of iron oxidation are Fe_2O_3, Fe_3O_4, goethite (α-FeOOH), akaganéite (β-FeOOH), and lepidocrocite (γ-FeOOH) (Figure 1(b)) (Ghosh *et al.* 2017).

Adsorption of nitrate followed by subsequent redox reaction is generally recognized as the principal mechanisms of the nitrate removal process by nZVI (Figure 1(b)) (Liu & Wang 2019). The possible end products of the nitrate reduction reaction by nZVI include nitrite, nitrogen gas, and ammonium (Figure 1(b)) (Khalil *et al.* 2016). However, Hwang & co-authors (2011) identify ammonium as the end product of nitrate reduction using nZVI, as shown in Equation (11).

$$2Fe^0_{(s)} + 4H^+_{(aq)} + O_{2(aq)} \rightarrow 2Fe^{2+} + 2H_2O_{(l)} \quad E_0 = +1.67V\ \Delta G^0 < 0 \tag{1}$$

$$2Fe^0_{(s)} + 2H_2O_{(l)} \rightarrow 2Fe^{2+} + H_{2(g)} + 2OH^-_{(aq)} \quad E_0 = -0.39V\ \ \Delta G^0 > 0 \tag{2}$$

$$2Fe^{2+}_{(s)} + 2H^+_{(aq)} + 0.5O_{2(aq)} \rightarrow 2Fe^{3+} + H_2O_{(l)} \quad E_0 = +0.46V\ \ \Delta G^0 < 0 \tag{3}$$

$$2Fe^{2+}_{(s)} + 2H_2O_{(l)} \rightarrow 2Fe^{3+} + H_{2(g)} + 2OH^-_{(aq)} \quad E_0 = -1.60V\ \ \Delta G^0 > 0 \tag{4}$$

$$Fe^{3+} + 3OH^- \rightarrow Fe(OH)_3 \downarrow \tag{5}$$

$$Fe(OH)_3 \rightarrow FeOOH \downarrow + H_2O \tag{6}$$

$$2Fe^0_{(s)} + O_2 \rightarrow 2FeO \tag{7}$$

$$6FeO + O_2 \rightarrow 2Fe_3O_4 \tag{8}$$

$$4Fe_3O_4 + O_2 \rightarrow 6Fe_2O_3 \tag{9}$$

$$2Fe^0 + O_2 + 2H_2O \rightarrow 2Fe^{2+} + 4OH^- \tag{10}$$

$$4Fe^0 + NO_3^- + 10H^+ \rightarrow 4Fe^{2+} + NH_4^+ + 3H_2O \quad \Delta Go = -997.71kJ/mol \tag{11}$$

Water Practice & Technology Vol 15 No 4
doi: 10.2166/wpt.2020.086

The effectiveness of nZVI in nitrate removal decreases sharply when exposed to the atmosphere because of the rapid formation of an oxide layer in the presence of DO affecting the reactivity of nZVI. Previous researchers have focused on the synthesis of nZVI particles under inert (no oxygen) conditions while purging nitrogen (N_2) or argon (Ar) gas to keep iron in its zerovalent state. Nevertheless, field applications are often plausible under oxic conditions; hence, synthesis under oxic conditions is pivotal to be examined. Besides, the recovery of spent nZVI nanoparticles is a major concern during field application in water treatment, as the presence of nanoparticles in the treated water is a health concern (Mukherjee *et al.* 2016). Thus, the magnetic property of nZVI particles could be harnessed in removing the spent nZVI particles from the solution after treatment. The magnetic properties of nZVI are known to facilitate the rapid separation of nZVI from water via the application of an external magnetic field (Huang *et al.* 2013). The novelty of this research is to study the effectiveness of nZVI synthesis and its use under oxic conditions for nitrate removal from nitrate-rich groundwater. The objectives of this study are, therefore, to investigate: (i) the possibility of synthesis of nZVI under ambient conditions in the presence of DO, (ii) the effectiveness of nZVI (synthesised under oxic conditions) on nitrate removal from nitrate-rich water under oxic conditions, (iii) the potential nitrate removal mechanisms under the oxic environment, and (iv) the percentage of spent nZVI particles that can be recovered from the solution using an external magnetic field.

MATERIALS AND METHODS

Chemical reagents

Analytical grade chemicals such as $FeCl_3$ (anhydrous, 98%, PARK Scientific Ltd, Northampton, UK), $NaBH_4$ (Crystals, extra pure, 98%, Sysco Research Laboratories, India), polyethylene glycol (PARK Scientific Ltd, Northampton, UK), ethanol (99.5%, Breckland Scientific Supplies, UK), and deionized water (SMART series Water Purification System, Shanghai Canrex Analytical Instrument Co. Ltd) were used for the synthesis of nZVI. Sodium nitrate (99%, DaeJung Chemicals & Metals Co. Ltd) was used to prepare the nitrate stock solution (1,000 mg/L).

Synthesis of nZVI

The nZVI was synthesized by the reduction of $FeCl_3$ using $NaBH_4$ following the method given by Khalil *et al.* (2016), with modifications as shown in Equation (12).

$$4Fe^{3+} + 3BH_4^- + 9H_2O \rightarrow 4Fe^0 + 3H_2BO_3^- + 12H^+ + 6H_2 \quad (12)$$

The $NaBH_4$ solution (625 ml of 0.18 N) was pipetted to the $FeCl_3$ solution (325 ml of 0.11 N), with a volumetric ratio of $NaBH_4$: $FeCl_3 = 1.9$: 1, using a burette and a 2,000 mL volumetric flask. The synthesized mixture was stirred at 350 rpm, kept at 25 $\pm$ 0.5 °C using an ice bath, and left for one hour while stirring to complete the reactions. After the reduction, the black iron nanoparticles (nZVI) were washed three times with ethanol, each followed by sonication for 15 minutes. The slurry was oven-dried at 100 °C for 12 hours before applied in batch experiments.

During the synthesis process of nZVI, nitrogen gas was not purged, as it would yield inert conditions. It was anticipated that trace levels of DO present in the open air during the synthesis of nZVI would not lead to complete oxidation of the nZVI shell during the synthesis process, and the reactivity would remain sufficient for effective nitrate removal. Such assumptions are supported by retrospective research in which Yuvakkumar *et al.* (2011) reported that nZVI particles synthesized

Water Practice & Technology Vol 15 No 4
doi: 10.2166/wpt.2020.086

(50–100 nm) in the presence of trace levels of DO under atmospheric conditions were mainly in zerovalent oxidation state. Also, noted was that this nZVI consisted of a zerovalent core surrounded by an oxide shell, and remained potent for weeks without significant oxidation.

Characterization of nZVI

The nZVI phase identification before and after the reaction was performed by X-ray Powder Diffraction (XRD) technique (XRD-D8, ECO, Advance Bruker Diffractometer with filtered Cu Kα radiation, Germany). The average size of crystallites synthesized (d) was determined using Scherrer's equation (Equation (13)), where Scherrer's constant is 0.89, λ is the wavelength of XRD, B is the full width at half maximum of the peak, and cos θ is the Bragg angle (Eljamal *et al.* 2018, 2019).

$$d = (0.89\lambda)/(B \cos \theta) \quad (13)$$

The morphology and elemental composition of nZVI were analyzed before and after the batch experiments, using Environmental Scanning Electron Microscopy (ESEM, Carl Zeiss, Evo 18, Secondary Electron Microscope, Germany) with Energy-Dispersive X-ray spectroscopy (EDAX, Element EDS system, AMETEK Materials Analysis Division, USA). Fourier transform-infrared spectroscopy (FT-IR, ALPHA Bruker, Germany) was performed in adsorption mode at ambient temperature in the spectral range of 400–4,000 cm^{-1} to identify the functional groups of nZVI.

Batch experiments on nitrate removal by nZVI

The removal of nitrate using nZVI was studied through batch experiments. A stock solution of nitrate (1,000 mg/L) was prepared using deionized water. For the batch experiments, a solution with 150 mg/L nitrate (as NO_3^-) concentration was prepared by diluting the stock solution using deionized water. Nitrate concentration of 150 mg/L was chosen for the study based on the nitrate levels reported in groundwater sources in Sri Lanka (Gunatilake & Iwao 2010; Gunatilake 2016; Nijamir & Kaleel 2017; Herath 2018).

Depending on the environmental conditions and numerous activities taking place in the watershed, potable groundwater can be contaminated with various natural and human-induced contaminants such as fluoride, hardness, iron, manganese, heavy metals, organic compounds, pesticides, and pathogenic microorganisms. The presence of these constituents simultaneously with nitrate can influence the reactivity of nZVI for nitrate removal. The main objective of this study is to investigate the effectiveness of nZVI synthesized under oxic conditions for nitrate removal and potential nitrate removal mechanisms by nZVI under the oxic environment. Hence, potable groundwater collected from the field was not used in the experiments. Instead, a synthetic water sample prepared in the laboratory using high purity chemical containing nitrate and deionized water was used for the experiments to minimize the possible interfering effects of other groundwater contaminants on the nitrate removal and reactivity of nZVI.

Determination of optimum nZVI dosage, the effect of contact time on nitrate removal, and nitrate removal pathways by nZVI

The nitrate reduction by nZVI was investigated in batch reactors at predetermined time intervals to find the optimum contact time and dosage of nZVI for the removal of nitrate to a level below 50 mg/L. The batch reactors were filled up to 250 mL with a nitrate solution (150 mg/L). Varying dosages of nZVI (250–10,000 mg/L) were added to the batch reactors. The solutions were continuously stirred at 250 rpm, room temperature of 25 $\pm$ 0.5 °C, and an initial pH of 5.5–5.7. At each sampling time (at 5, 15, 30, 60, 120, and 240 minutes), samples were filtered four times through

Water Practice & Technology Vol 15 No 4
doi: 10.2166/wpt.2020.086

filter papers with 11 μm pore size, and the filtrates were analyzed for residual nitrate levels and ammonium ion concentrations. All batch experiments were conducted under oxic conditions. A control experiment was conducted under similar experimental conditions in the absence of nZVI particles. All experiments were conducted in duplicates. The mean values and standard deviations were calculated based on the duplicate measurements and the results were compared to determine the optimum nZVI dosage and contact time.

The possibility of a loss of nitrogen mass from the aqueous phase because of ammonia stripping to the gas phase can be elaborated by determining the fraction of dissolved un-ionized ammonia in the solution under the experimental conditions. The relationship between relative concentrations of ammonium and ammonia in aqueous solution can be described by Equation (14) (Erickson 1985).

$$K_a = [NH_3][H^+]/[NH_4^+] \tag{14}$$

where K_a is the acid dissociation constant for ammonium, $[NH_3]$ is the dissolved ammonia concentration in the solution, $[H^+]$ is the H^+ concentration in the solution, and $[NH_4^+]$ is the ammonium concentration in the solution.

Further, the relative concentrations of ammonium and ammonia present in the nitrate/nZVI system are temperature-dependent, as shown in Equation (15) (Emerson *et al.* 1975). The dissolved un-ionized fraction of ammonia can be calculated with measured pH and temperature of the solution using Equation (16) (Clément & Merlin 1995).

$$pK_a = 0.09018 + 2729.92/(273.2 + T) \tag{15}$$

where T is the temperature of the solution (°C) and pK_a is the negative log of the acid dissociation constant for ammonium.

$$\text{Un-ionized } NH_3(\%) = 100/[1 + 10^{(pKa-pH)}] \tag{16}$$

where pK_a is the negative log of the acid dissociation constant for ammonium, pH is the solution pH at a given reaction time.

Removal of the spent nZVI particles using an external magnetic field

The potential of an external magnetic field, coupled with the inherent magnetic properties of nZVI particles, was investigated for the removal of spent nZVI particles from the solution after treatment. Neodymium magnet balls (3-mm diameter, N38 grade, the strength of 2,000 G, weight 0.1074 g) were used as the external magnetic field. These neodymium magnet balls (432 balls) were placed on a conical shape glass funnel containing a filter paper (pore size 11 μm). At the end of the 30-minute contact time, the reaction solution (nitrate and nZVI) was filtered through the arrangement with magnet balls at a flow rate of 10 mL/min. The filtrate was collected in polypropylene centrifuge tubes (15 mL) and centrifuged at 3,500 rpm for 10 minutes. The supernatant in the centrifuge tubes was checked for the presence of any nZVI particle residuals to determine the extent of nZVI particle removal during filtration through the funnel with magnet balls. The weights of the filter paper and conical shape funnel made of Neodymium magnet balls were measured before and after filtering the mixture (nitrate solution and nZVI) using a 5-digit analytical balance. Before measuring the weight after filtration, the filter paper and conical shape funnel made of Neodymium magnet balls were dried in an oven while purging oxygen-free nitrogen gas to eliminate the entrapped moisture in the setup. The drying process was carried out in an oxygen-free environment to avoid further oxidation and possible changes in the weight of nZVI particles. Such weight measurements were used to determine the

Water Practice & Technology Vol 15 No 4
doi: 10.2166/wpt.2020.086

recovery of nZVI particles from the solution, possible losses, and escape from nZVI to the filtrate, and efficiency of magnet balls for nZVI removal.

Analytical methods

The nitrate concentrations in the solution were determined using the Ion Chromatography (Compact Ion Chromatography system, Metrohm, 930 Compact IC Flex, Switzerland) with a mobile phase of 3.2 mmol/L Na_2CO_3 + 1 mmol/L $NaHCO_3$, the flow rate of 0.7 m/L/min, and level of detection being 0.02 mg/L. Total ammonium ion concentration in the solution was measured using the preliminary distillation step (sample volume 200 ml) (4500-NH_3 B. Preliminary distillation step) followed by a titrimetric method (4500-NH_3 C. Titrimetric method), as given in Standard Methods for the Examination of Water and Wastewater (23rd edition) (APHA 2017). Preliminary distillation was carried out using UDK 149 Automatic Kjeldahl Distillation Unit (VELP Scientifica, USA). Distillation was done at a rate of 6–10 mL/min, and the distillate was collected in a flask containing a boric acid solution (0.32 N). The ammonium ions captured in the boric acid solution were quantified by titration with a sulphuric acid solution (0.02 N) using the mixed indicators (methylene blue + methyl red) (level of detection 0.5 mg/L). The pH of the reaction solution samples was measured using a pH meter (pH 2700 Eutech instruments, India). The mass of the conical funnel filled with Neodymium magnet balls was measured before and after filtration of the reaction solution, using a 5-digit semi-micro balance (EX125D, Explorer series, Ohasus Corporation, USA, maximum capacity 120 g, readability 0.00001 g).

RESULTS AND DISCUSSION

Characterization of nZVI

XRD analysis

The XRD analysis carried out on the nZVI samples before treatment (Figure 2) confirmed the formation of nZVI with diffraction peaks at 44.7° (110) and 65.1° (200) (Sohrabi *et al.* 2014; Zhang *et al.* 2017; Wei *et al.* 2018). Also, the diffraction peaks at 30.3° (220), 35.7° (311), 43.7° (400), 57.4° (511), and 63.1° (440) (Figure 2) represent the existence of maghemite-γFe_2O_3/magnetite-Fe_3O_4 (Liu *et al.* 2014a, 2014b; Eljamal *et al.* 2018, 2019; Wei *et al.* 2018). Such a formation was a result of oxidation of nZVI by water and oxygen because the nZVI was synthesized in the presence

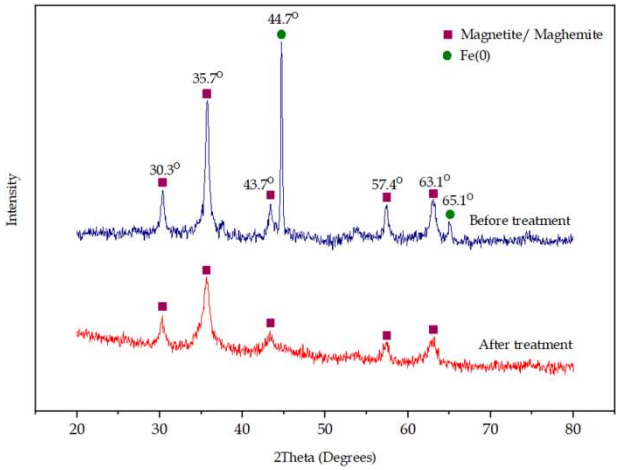

Figure 2 | XRD spectra of nZVI before and after treatment with nitrate.

Water Practice & Technology Vol 15 No 4
doi: 10.2166/wpt.2020.086

of oxygen (Mu *et al.* 2017). The co-existence of nZVI and maghemite/magnetite in the nZVI sample before treatment provides evidence of the presence of a core-shell structure where the shell is predominantly composed of iron oxides by the oxidation of nZVI, and the core is made of Fe^0 because there is no oxidation (Hwang *et al.* 2011). The average crystallite size obtained for the synthesized nZVI particles was 33 nm (Equation (13)), which was within the nanoscale range (1–100 nm).

The XRD spectrum of nZVI after treatment (240-minute contact time) shows diffraction peaks at 30.3° (220), 35.7° (311), 43.7° (400), 57.4° (511), and 63.1° (440) (Figure 2). These peaks indicate the presence of maghemite-γFe_2O_3/magnetite-Fe_3O_4 on nZVI after treatment. The absence of nZVI characteristic diffraction peaks at 44.7° (110) and 65.1° (200) after treatment (Figure 2) was attributed to aspects such as the transformation of nZVI to magnetite and complete oxidation of nZVI to magnetite/maghemite (Hwang *et al.* 2011), possibly due to the oxic conditions prevalent during the nitrate reduction.

ESEM-EDAX analysis

The ESEM-EDAX analysis of nZVI was conducted before and after treatment to investigate the surface morphology and elemental distribution of nZVI (Figures 3 and 4). The ESEM image of nZVI before treatment (Figure 3(a)) shows that the nZVI particles were agglomerated in the form of ball-like structures connected with each other. The agglomeration observed in nZVI particles could be because of the high magnetic potency of the nZVI particles (Sohrabi *et al.* 2014; Ghosh *et al.* 2017). The EDAX analysis of nZVI before treatment (Figure 4(a)) manifests the presence of O (25%) and Fe (75%) as primary elements, and Cl (0.05%) is observed as an impurity because of the use of $FeCl_3$ for the synthesis of the nZVI particles.

The ESEM image of nZVI after treatment depicts an irregular texture with discernible cloudiness

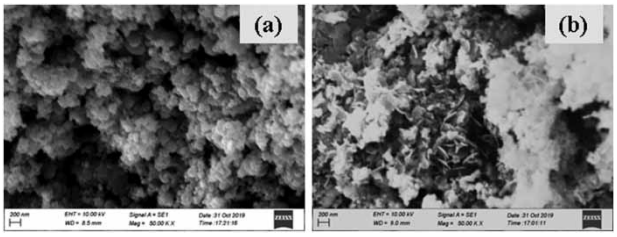

Figure 3 | ESEM images of nZVI (a) before treatment with nitrate and (b) after treatment with nitrate.

introduced to the combination of ball-like structures and newly formed flake-like structures, removing the sharpness of the ball-like structures (Figure 3(b)). The change in the surface morphology from sharp ball-like structures to irregular texture is attributed to the formation and deposition of various iron oxides on the nZVI. The characteristics of EDAX analysis (Figure 4(b)) indicate O (27%) and Fe (68%) as primary elements with Cl (0.7%) and Na (5%) as impurities. Elemental Na detected in the sample is because of the use of $NaNO_3$ for preparing the nitrate stock solution. The Fe content in nZVI decreased from 75% to 68% after treatment, which is ascribed to the oxidation of nZVI as a reductant during the reaction forming Fe^{2+} or Fe^{3+} (iron oxide or hydroxide) that are soluble ions in the solution (Fu *et al.* 2015).

FT-IR analysis

The FT-IR spectra of nZVI before and after treatment are shown in Figure (5). The band around 3,417 cm^{-1} of the FT-IR spectra of nZVI before treatment (curve (a) of Figure 5) is attributed to -OH vibration in H_2O molecules (Dong *et al.* 2017), indicating that some hydroxyl groups existed

Water Practice & Technology Vol 15 No 4
doi: 10.2166/wpt.2020.086

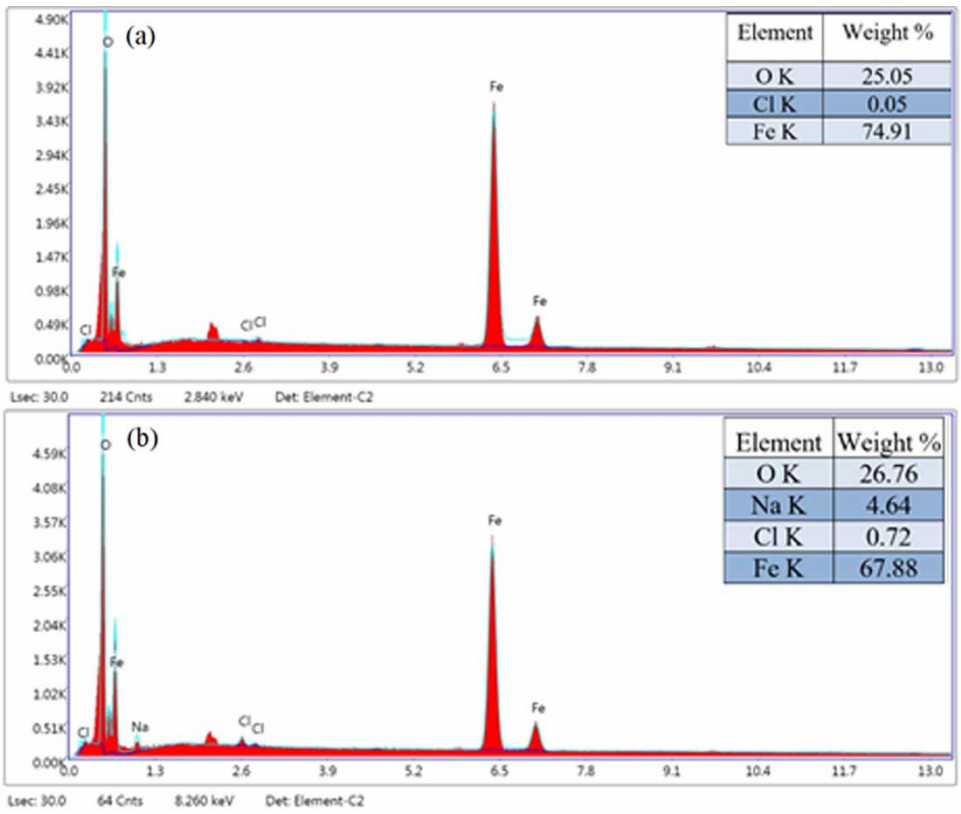

Figure 4 | EDAX spectrum of nZVI (a) before treatment with nitrate and (b) after treatment with nitrate.

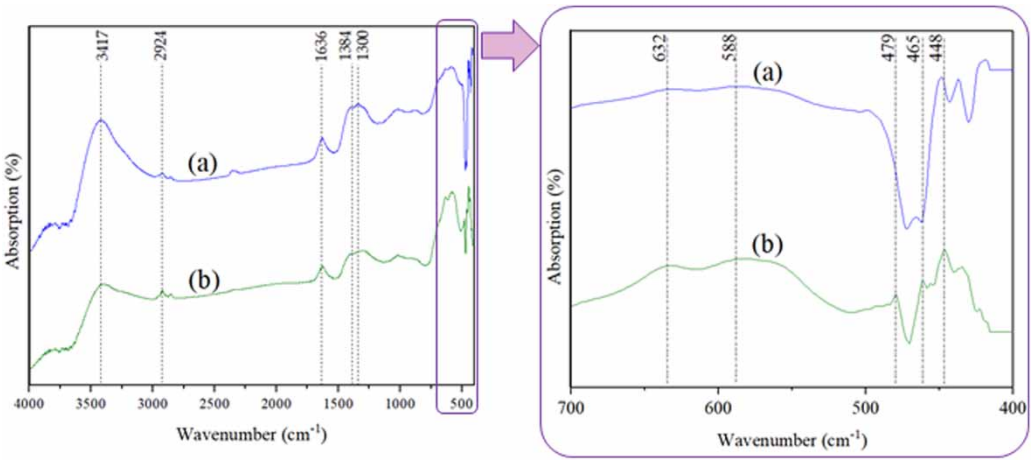

Figure 5 | FT-IR spectra of nZVI (a) before treatment with nitrate and (b) after treatment with nitrate.

on the surface of the nZVI sample. The vibrational band at 2,924 cm^{-1} (curve (a) of Figure 5) is attributed to the symmetric CH_2 stretching vibrations (Li *et al.* 2018), which is due to the use of ethanol in preparing nZVI. The band at 1,636 cm^{-1} (curve (a) of Figure 5) is ascribed to the absorption of water (Salama *et al.* 2015; Gao *et al.* 2016). The band around 1,300 cm^{-1} (curve (a) of Figure 5) is because of the ethanol used in preparing the nZVI sample (Kim *et al.* 2013). The bands at 588, 465, and 448 cm^{-1} (curve (a) of Figure 5) are attributed to magnetite/maghemite, hematite, and maghemite, respectively (Andrade *et al.* 2009). The FT-IR analysis of nZVI before treatment provides evidence and confirms the formation/presence of an iron oxide layer as a shell structure on the nZVI surface.

Water Practice & Technology Vol 15 No 4
doi: 10.2166/wpt.2020.086

The FT-IR analysis of nZVI after treatment exhibits changes in the spectrum compared to the same before treatment (curve (b) of Figure 5). The band at 3,397 cm^{-1} (curve (b) of Figure 5) is attributed to –OH vibration, which are Goethite-OH stretching bands (Salama *et al.* 2015). The vibrational bands at 2,923 and 1,636 cm^{-1} (curve (b) of Figure 5) remain similar to the same before treatment (curve (a) of Figure 5) because of the use of ethanol in preparing nZVI and absorption of water. The band around 1,300 cm^{-1} (curve (b) of Figure 5) is attributed to the ethanol used in preparing the nZVI sample (Kim *et al.* 2013). The new band at 632 cm^{-1} (curve (b) of Figure 5) is attributed to the presence of another iron oxide, β-FeOOH (Andrade *et al.* 2009), by the oxidation of nZVI as a result of nitrate reduction in the presence of oxygen. The band at 583 cm^{-1} (curve (b) of Figure 5) is assigned to magnetite/maghemite. The new band at 479 cm^{-1} (curve (b) of Figure 5) is assigned to the presence of another iron oxide, hematite (αFe_2O_3) (Andrade *et al.* 2009), by the oxidation of nZVI in the presence of oxygen. The band at 446 cm^{-1} (curve (b) of Figure 5) is attributed to maghemite (Andrade *et al.* 2009). Hence, the FT-IR analysis of nZVI particles after treatment provides evidence and confirms the oxidation of nZVI during nitrate reduction in the presence of oxygen and formation/presence of various iron oxides other than magnetite/maghemite forming the shell structure on the nZVI surface.

Effect of initial nZVI dosage and contact time on optimum nitrate removal

The batch experiments were conducted for varying dosages of nZVI (250–10,000 mg/L) with nitrate (150 mg/L), the contact time of two hours, pH of 5.5, and ambient water temperature of 24 °C. For several dosages of nZVI, the residual nitrate levels in batch reactors after two hours are shown in Figure 6. When nZVI dosages were 250 and 500 mg/L, the final nitrate concentrations in the solution did not reach the permissible level of 50 mg/L after a two-hour contact time (data not shown in Figure 6). This could have been because of the low stoichiometric excess of Fe^0 concentrations in the batch reactors (Choe *et al.* 2000). When the nZVI dosage was 1,000 mg/L, the nitrate removal efficiency increased to 91%, with the residual nitrate level being 13 mg/L after two-hour contact time (Figure 6). With 1,000 mg/L nZVI dosage, the remaining nitrate concentration reached 30.3 mg/L after a 30-minute reaction time (80% removal efficiency) (Figure 6), which is less than the WHO/SLS permissible level of 50 mg/L for drinking water.

With the increase of nZVI dosages beyond 1,000 mg/L, the amount of nitrate removed decreased significantly (Figure 6). For nZVI dosage of 2,000 mg/L, more than one hour was required to reach

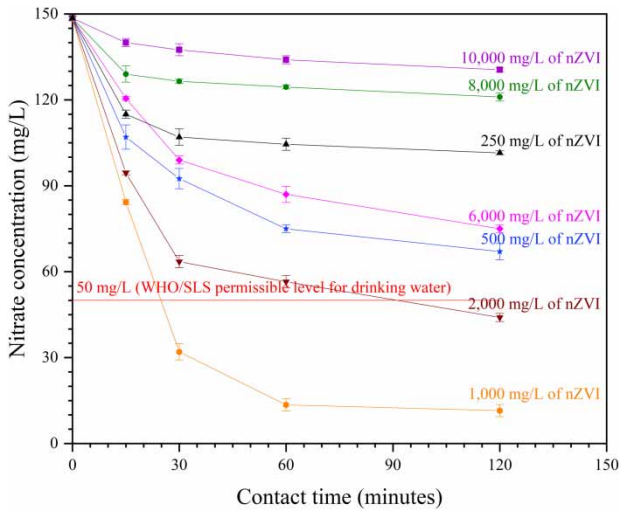

Figure 6 | Effect of contact time and nZVI concentration on nitrate reduction under oxic conditions.

Water Practice & Technology Vol 15 No 4
doi: 10.2166/wpt.2020.086

the nitrate level of 50 mg/L (Figure 6). For nZVI dosages higher than 2,000 mg/L, the final nitrate concentration did not reach a value below 50 mg/L within a contact time of two hours. Lower nitrate reduction ability for high nZVI dosages (>1,000 mg/L) may have been influenced by a higher degree of agglomeration affinity propelled by elevated van der Waals and magnetic attraction forces resulting in a loss of available reactive sites for nitrate removal (Litter *et al.* 2018).

Following the observations mentioned above, a contact time of 30 minutes was selected as the optimum contact time with an optimum nZVI dosage of 1,000 mg/L (Figure 6). The findings of the present study showed 80% nitrate removal efficiency (at 30 minutes contact time) under aerobic conditions when using 1,000 mg/L nZVI dosage, which is synthesized under oxic conditions. Previous studies have focused on nitrate removal using the nZVI synthesised in the absence of oxygen to keep iron in its zerovalent state, anticipating high nZVI reactivity and nitrate removal. For example, Khalil *et al.* (2016) used the nZVI (2,000 mg/L) synthesized under anaerobic conditions and reported only 40% nitrate removal efficiency at 30 minutes of contact time under aerobic conditions. Therefore, our results corroborate that the reactivity of nZVI used in the present study has not been affected by the presence of oxygen during the nZVI synthesis process and resulted in superior nitrate removal efficiency under aerobic conditions compared to the nitrate removal reported under aerobic conditions using nZVI synthesized under anaerobic conditions.

This study was carried out using an artificial nitrate contaminated water sample prepared in the laboratory. However, potable groundwater may contain various other natural and human-induced contaminants such as cations, anions, organic ligands, hardness, pesticides, and pathogenic microorganisms. Such constituents are likely to have an impact on the reactivity of nZVI for nitrate removal because of (1) competition created by co-contaminants for the same reactive sites of nZVI, (2) changing the structure and chemical composition of the oxide shell with the formation of a passivating oxide layer blocking the reactive sites, and (3) change in the rate of dissolution of the iron oxide shell increasing the reductive potential (Mu *et al.* 2017). Hence, the performance of nZVI may vary when the artificial nitrate contaminated water sample is replaced by a potable groundwater sample collected from the field. The presence of organic acids such as formic acid, oxalic acid, and citric acid has shown retardation of the nitrate reduction by nZVI with the order of formic acid > oxalic acid > citric acid because of the high affinity of organic ligands to adsorb on the iron oxide shell of nZVI decreasing the availability of active sites for nitrate reduction (Mu *et al.* 2017). Halide anions such as chloride and bromide are known to be pitting and crevice corrosion promoters; hence, their presence could result in the dissolution of passive oxide shells leading to prolonged reactivity of nZVI for nitrate removal (Mu *et al.* 2017).

Nitrate reduction reaction pathways by nZVI

The batch study was continued for an extended contact time of four hours to observe the complete removal of nitrate from the solution and to investigate the possible pathways that contributed to nitrate removal by nZVI from the solution under oxic conditions with the following settings: the initial nitrate concentration of 150 mg/L, nZVI dosage of 1,000 mg/L, pH of 5.5, mixing speed of 250 rpm, and at an ambient water temperature of 24 °C, (Figure 7). During the experiment, ammonium was detected as the major end product in the solution (Figure 7), with ammonium levels in the range of 19 mg/L (at 15 minutes) to 30 mg/L (at 240 minutes). The total theoretical amount of nitrogen present in the initial nitrate solution with 150 mg/L corresponds to about 34 mg-nitrogen/L.

After a 15-minute contact time, nitrogen mass balance showed that the nitrogen mass was 100% conserved in the solution with partitioning to different nitrogen components, mainly nitrate (19 mg nitrogen/L) and combined ammonium + ammonia (15 mg nitrogen/L). Although the nitrate ions can entrap in the pores of the nZVI core structure (Mu *et al.* 2017), it was assumed that the loss of nitrogen due to nitrate ions entrapping in the pores of nZVI core structure during the reaction

Water Practice & Technology Vol 15 No 4
doi: 10.2166/wpt.2020.086

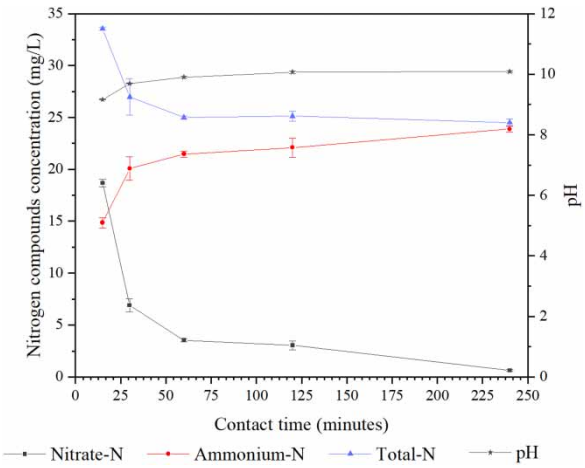

Figure 7 | Concentration of nitrogen compounds and pH variation in the solution.

period was negligible. Hence, a 1:1 stoichiometric ratio was determined for the transformation of nitrate to ammonium. The reaction between nZVI and nitrate can, therefore, follow the reaction pathway, as indicated in Equation (11), that it is more thermodynamically favorable to produce ammonium ions (Hwang *et al.* 2010).

During the 4-hour reaction period, the nitrate concentration in the solution continuously decreased (Figure 7). At the optimum contact time of 30 minutes, only 80% nitrogen mass balance was achieved (27 mg nitrogen/L; the sum of the total nitrogen-containing species in the solution), indicating a 20% loss of nitrogen in the system (7 mg nitrogen/L) (Figure 7). After 60-minute contact time, the measured ammonium concentration in the solution remained almost constant (Figure 7). The nitrogen mass balance for reaction times of 60–240 minutes were in the range of 73–70%, respectively, resulting in about 27–30% loss of nitrogen in the system (Figure 7). The loss of nitrogen mass in the system after 15 minutes was attributed to ammonia stripping to the gas phase leading to a reduction in nitrogen-containing species in the solution. In the present study, the formation of ammonium during the reaction of nitrate with nZVI increased the solution pH (from initial solution pH 5.5 to final solution pH 10.1 after 4 hours) (Figure 7) and ammonia stripping is evident when the solution pH is greater than 9.5 (Khalil *et al.* 2016). Similar observations were reported by previous research where, during nitrate removal by nZVI, the ammonia stripping occurred at solution pH $>$ 9.5 (Hwang *et al.* 2010; Hwang *et al.* 2011; Khalil *et al.* 2016).

In the present study, pKa at 24 °C was determined using Equation (15) and found to be 9.28. Further, the fraction of un-ionized ammonia (%) present in the solution at each reaction time was calculated using Equation (16) (Figure 8). At 30-minute contact time under the conditions of pH 9.7 and temperature of 24 °C, the fraction of un-ionized ammonia was found to be 72% (Figure 8). Hence, under the prevailing experimental conditions, at 30-minute contact time, 72% of the nitrogen is available in the form of un-ionized ammonia dissolved in the solution. Similarly, the un-ionized ammonia fraction in the solution from 60 to 240 minutes was determined as 81–87%, respectively (Figure 8). However, only a fraction of the dissolved amount can be stripped because of factors such as (i) the solution pH has not reached a high pH level (e.g. pH 11–12) that can cause the change of the ratio of NH_3/NH_4^+ in favor of NH_3 gas for effective ammonia stripping, and (ii) low surface area to volume ratio available in the batch reactor hindering ammonia gas stripping (Hossini *et al.* 2016).

Physical separation of nZVI particles from the solution using magnetism

The strong magnetic property of nZVI was utilized to separate the spent nZVI particles from the reaction solution after the treatment. A funnel made of Neodymium magnet balls (diameter: 3 mm) was

Water Practice & Technology Vol 15 No 4
doi: 10.2166/wpt.2020.086

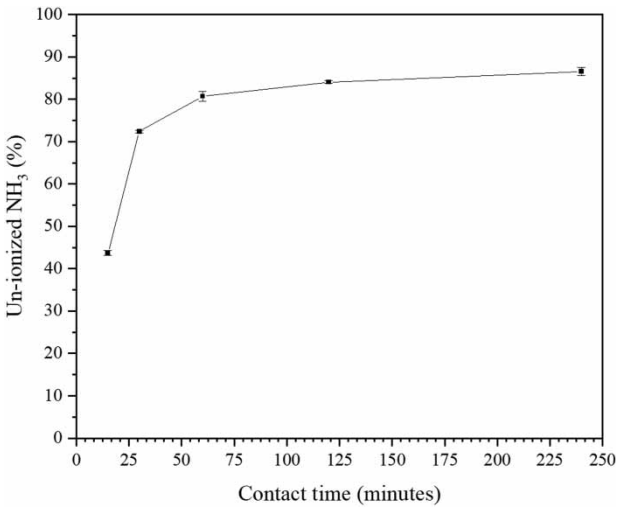

Figure 8 | Un-ionized NH_3 (%) in the solution.

used, as shown in Figure 9(a). At the end of the 30-minute reaction, the solution (nitrate/nZVI) (Figure 9(a)) was filtered through the funnel with the magnet balls (Figure 9(b)), and the filtrate was centrifuged at 3,500 rpm. It was observed that the nZVI particles retained on the magnet balls (Figure 9(c)). Any residual fraction of nZVI particles was not observed at the bottom of the centrifuge tube after centrifugation (Figure 9(d)), indicating that all nZVI particles were retained by magnet balls (w/w) (Figure 9(b) and 9(c)). The weight of the filter paper and conical-shape funnel made of Neodymium magnet balls was measured before and after filtering the mixture (nitrate solution and nZVI) using a 5-digit analytical balance, to confirm the maximum recovery of the nZVI particles from the treated water. The weight measurements proved that 99.9% of the initial nZVI mass used in the experiment was recovered via filtering through the filter arrangement made with magnet balls. Thus, the findings showed that the magnetism of nZVI facilitates the physical separation of the nZVI from treated water when using an external magnetic field.

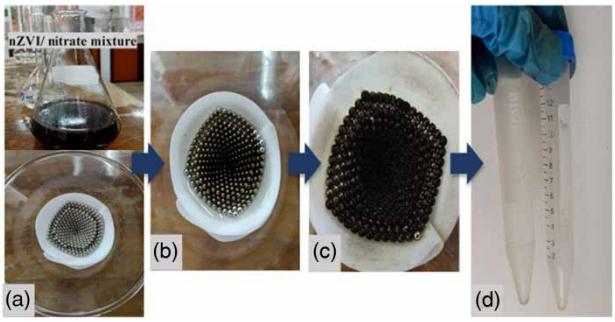

Figure 9 | Physical separation of spent nZVI particles using magnet balls and filtration.

The rapid separation of nZVI particles from the solution when filtering through the external magnetic field was attributed to the presence of a combined matrix of nZVI and iron oxides (magnetite/maghemite) on the nZVI particles after the reaction. The XRD (Figure 1) and FT-IR (Figure 4) analyses confirmed that nZVI after treatment contained a combination of nZVI and Fe_3O_4. The magnetism of the mixed composition is attributed to nZVI and Fe_3O_4, of which the latter has been reported to have a stronger propensity than that observed with nZVI or Fe_3O_4 alone (Lu *et al.* 2016).

Water Practice & Technology Vol 15 No 4
doi: 10.2166/wpt.2020.086

CONCLUSIONS

The nitrate removal from groundwater sources can be carried out effectively under oxic conditions with 1,000 mg/L of nZVI dosage within 30 minutes to a level less than the WHO and SLS permissible level for drinking water (50 mg/L), where the initial nitrate concentration of the sample was 150 mg/L. The ammonium ion was the major product of the reduction reaction followed by ammonia stripping, which occurred at basic pH ($pH > 9.5$) values. Ammonia stripping can be considered as the reason for the total nitrogen loss, which was observed after a 30-minute reaction time. Further, the removal of used nZVI from treated water can be effectively achieved by filtering the solution through an external magnetic field. Thus, the use of nZVI synthesized under oxic conditions is a reliable and effective method to remove excess levels of nitrate from nitrate-contaminated groundwater under oxic conditions. The reusability potential of spent nZVI material recovered using the external magnetic field could be worthy of exploring in the future. In conclusion, nZVI synthesized under oxic conditions can be effectively utilized in the presence of oxygen for removal of nitrate from groundwater contaminated with excessive nitrate levels, to levels that are safe for drinking, with minimum control measures to maintain inert conditions.

ACKNOWLEDGEMENT

The authors would like to acknowledge the financial support provided by the University of Moratuwa, Sri Lanka and the National Research Council (NRC), Sri Lanka (Grant No. 15-056) as well as the analytical support extended by the Department of Material Science and Engineering, University of Moratuwa, Sri Lanka.

DATA AVAILABILITY STATEMENT

Data cannot be made publicly available; readers should contact the corresponding author for details.

REFERENCES

Afkhami, A., Madrakian, Z. & Karimi, Z. 2007 The effect of acid treatment of carbon cloth on adsorption of nitrite and nitrate ions. *J. Hazard. Mater.* **144**, 427–431.

Andrade, A. L., Souza, D. M., Pereira, M. C., Fabris, J. D. & Domingues, R. Z. 2009 Synthesis and characterization of magnetic nanoparticles coated with silica through a sol-gel approach. *Cerâmica* **55**(336), 420–424. https://doi.org/10.1590/S0366-69132009000400013.

APHA 2017 *Standard Methods for the Examination of Water and Wastewater* 23rd edn. American Public Health Association/American Water Works Association/Water Environment Federation, Washington, DC, USA.

Archna, Sharma, S. K. & Sobti, R. C. 2012 Nitrate removal from ground water: a review. *E-J. Chem.* **9**(4), 1667–1675. https://doi.org/10.1155/2012/154616.

Arora, M., Eddy, N. K., Mumford, K. A., Baba, Y., Perera, J. M. & Stevens, G. W. 2010 Surface modification of natural zeolite by chitosan and its use for nitrate removal in cold regions. *Cold Reg. Sci. Technol.* **62**(2–3), 92–97. doi:10.1016/j.coldregions.2010.03.002.

Babuponnusami, A. & Muthukumar, K. 2012 Removal of phenol by heterogenous photo electro Fenton-like process using nano-zero valent iron. *Sep. Purif. Technol.* **98**, 130–135. doi:10.1016/j.seppur.2012.04.034.

Bawatharani, R., Mowjood, M. I. M., Dayawansa, N. D. K. & Kumaragamage, D. 2004 Nitrate leaching as a function of fertilization and irrigation practices in sandy regosols. *Trop. Agric. Res.* **16**, 172–180.

Bhatnagar, A., Kumar, E. & Sillanpää, M. 2010 Nitrate removal from water by nano-alumina: characterization and sorption studies. *Chem. Eng. J.* **163**, 317–323. doi:10.1016/j.cej.2010.08.008.

Chatterjee, S. & Woo, S. H. 2009 The removal nitrate from aqueous solutions by chitosan hydrogel beads. *J. Hazard. Mater.* **164**, 1012–1018. doi:10.1016/j.hazmat.2008.09.001.

Choe, S., Chang, Y.-Y., Hwang, K.-Y. & Khim, J. 2000 Kinetics of reductive denitrification by nanoscale zero-valent iron. *Chemosphere* **41**(8), 1307–1311. doi:10.1016/s0045-6535(99)00506-8.

Water Practice & Technology Vol 15 No 4
doi: 10.2166/wpt.2020.086

Clément, B. & Merlin, G. 1995 The contribution of ammonia and alkalinity to landfill leachate toxicity to duckweed. *Sci. Total Environ.* **170**(1–2), 71–79. https://doi.org/10.1016/0048-9697(95)04563-G.

Cornell, R. M. & Schwertmann, U. 2003 *The Iron Oxides: Structure, Properties, Reactions, Occurences and Uses*, 1st edn. John Wiley & Sons, Hoboken, NJ, USA. https://doi.org/10.1002/3527602097.

Diao, M. & Yao, M. 2009 Use of zero-valent iron nanoparticles in inactivating microbes. *Water Res.* **43**(20), 5243–5251. doi:10.1016/j.watres.2009.08.051.

Dong, H., Deng, J., Xie, Y., Zhang, C., Jiang, Z., Cheng, Y., Hou, K. & Zeng, G. 2017 Stabilization of nanoscale zero-valent iron (nZVI) with modified biochar for Cr (VI) removal from aqueous solution. *J. Hazard. Mater.* **332**, 79–86. http://dx.doi.org/doi:10.1016/j.jhazmat.2017.03.002.

Eljamal, O., Jinno, K. & Hosokawa, T. 2008 Modeling of solute transport with bioremediation processes using sawdust as a matrix. *Water Air Soil Pollut.* **195**, 115–127. doi:10.1007/s11270-008-9731-y.

Eljamal, O., Thompson, I. P., Maamoun, I., Shubair, T., Kareman, E., Lueangwattanapong, K. & Sugihara, Y. 2019 Investigating the design parameters for a permeable reactive barrier consisting of nanoscale zero-valent iron and bimetallic iron/copper for phosphate removal. *J. Mol. Liq.* **299**, 112144. https://doi.org/10.1016/j.molliq.2019.112144.

Eljamal, R., Eljamal, O., Khalil, A. M. E., Saha, B. B. & Matsunaga, N. 2018 Improvement of the chemical synthesis efficiency of nano-scale zero-valent iron particles. *J. Environ. Chem. Eng.* **6**(4), 4727–4735. https://doi.org/10.1016/j.jece.2018.06.069.

Elshafai, M., Hamdy, A. & Hefny, M. 2018 Zero-valent iron nanostructures: synthesis, characterization and application. *J. Environ. Biotechnol. Res.* **7**(1), 1–10.

Emerson, K., Russo, R. C., Lund, R. E. & Thurston, R. V. 1975 Aqueous ammonia equilibrium calculations: effect of pH and temperature. *J. Fish. Res. Board Can.* **32**(12), 2379–2383. http://dx.doi.org/10.1139/f75-274.

Erickson, J. R. 1985 An evaluation of mathematical models for the effect of pH and temperature on ammonia toxicity to aquatic organisms. *Water Res.* **19**(8), 1047–1058. https://doi.org/10.1016/0043-1354(85)90375-6.

Esfahani, A. R., Firouzi, A. F., Sayyad, G., Kiasat, A., Alidokht, L. & Khataee, A. R. 2014 Pb(II) removal from aqueous solution by polyacrylic acid stabilized zero-valent iron nanoparticles: process optimization using response surface methodology. *Res. Chem. Intermed* **40**, 431–445. https://doi.org/10.1007/s11164-012-0975-1.

Fan, J., Guo, Y., Wang, J. & Fan, M. 2009 Rapid decolorization of azo dye methyl orange in aqueous solution by nanoscale zerovalent iron particles. *J. Hazard. Mater.* **166**(2–3), 904–910. https://doi.org/10.1016/j.jhazmat.2008.11.091.

Fang, Z., Chen, J., Qiu, X., Cheng, W. & Zhu, L. 2011 Effective removal of antibiotic metronidazole from water by nanoscale zero-valent iron particles. *Desalination* **268**(1–3), 60–67. https://doi.org/10.1016/j.desal.2010.09.051.

Fu, R., Yang, Y., Xu, Z., Zhang, X., Guo, X. & Bi, D. 2015 The removal of chromium (VI) and lead (II) from groundwater using sepiolite-supported nanoscale zero-valent iron (S-NZVI). *Chemosphere* **138**, 726–734. http://dx.doi.org/10.1016/j.chemosphere.2015.07.051.

Gao, J.-F., Li, H.-Y., Pan, K.-L. & Si, C.-Y. 2016 Green synthesis of nanoscale zero-valent iron using a grape seed extract as stabilizer agent and the application for quick decolorization of azo and anthraquinone dyes. *RSC Adv.* **6**(27), 22526–22537. https://doi.org/10.1039/C5RA26668H.

Ghauch, A., Tuqan, A. & Assi, H. A. 2009 Antibiotic removal from water: elimination of amoxicillin and ampicillin by microscale and nanoscale iron particles. *Environ. Pollut.* **157**(5), 1626–1635. doi:10.1016/j.envpol.2008.12.024.

Ghosh, A., Dutta, S., Mukherjee, I., Biswas, S., Chatterjee, S. & Saha, R. 2017 Template-free synthesis of flower-shaped zero-valent iron nanoparticle: role of hydroxyl group in controlling morphology and nitrate reduction. *Adv. Powder Technol.* **28**(9), 2256–2264. http://dx.doi.org/10.1016/j.apt.2017.06.006.

Gunatilake, S. K. 2016 N and P variation in groundwater in wet zone and dry zone in Sri Lanka due to fertilization of paddy crop. *Int. J. Sci. Res. Publ.* **6**(9), 5.

Gunatilake, S. K. & Iwao, Y. 2010 A comparison of nitrate distribution in shallow groundwater of two agricultural areas in Sri Lanka and in Japan. *Sabaragamuwa Univ. J.* **9**(1), 81–95. http://doi.org/10.4038/suslj.v9i1.3736.

Herath, H. M. A. S. 2018 *Public Health and Groundwater Quality in Sri Lanka and Defluoridation of Drinking Water in Relation to Chronic Kidney Disease of Unknown Etiology*. PhD Thesis, Toyama Prefectural University, Imizu, Toyama Prefecture, Japan.

Hossini, H., Rezaee, A., Ayati, B. & Mahvi, A. H. 2016 Off-gas treatment of ammonia using a diffused air stripper: a kinetic study. *Health Scope* **5**(1), e26479. https://doi.org/10.17795/jhealthscope-26479.

Huang, Y. H. & Zhang, T. C. 2005 Effects of dissolved oxygen on formation of corrosion products and concomitant oxygen and nitrate reduction in zero-valent iron systems with or without aqueous Fe^{2+}. *Water Res.* **39**(9), 1751–1760. https://doi.org/10.1016/j.watres.2005.03.002.

Huang, P., Ye, Z., Xie, W., Chen, Q., Li, J., Xu, Z. & Yao, M. 2013 Rapid magnetic removal of aqueous heavy metals and their relevant mechanisms using nanoscale zero valent iron (nZVI) particles. *Water Res.* **47**(12), 4050–4058. https://doi.org/10.1016/j.watres.2013.01.054.

Hwang, Y. H., Kim, D. G., Ahn, Y. T., Moon, C. M. & Shin, H. S. 2010 Fate of nitrogen species in nitrate reduction by nanoscale zero valent iron and characterization of the reaction kinetics. *Water Sci. Technol.* **61**(3), 705–712. https://doi.org/10.2166/wst.2010.895.

Hwang, Y.-H., Kim, D.-G. & Shin, H.-S. 2011 Mechanism study of nitrate reduction by nano zero valent iron. *J. Hazard. Mater.* **185**(2–3), 1513–1521. doi:10.1016/j.jhazmat.2010.10.078.

Jensen, V. B., Darby, J. L., Seidel, C. & Gorman, C. 2012 *Drinking Water Treatment for Nitrate. Technical Report 6 in: Addressing Nitrate in California's Drinking Water with A Focus on Tulare Lake Basin and Salinas Valley Groundwater.*

Water Practice & Technology Vol 15 No 4
doi: 10.2166/wpt.2020.086

Report for the State Water Resources Control Board Report to the Legislature. Center for Watershed Sciences, University of California, Davis, CA.

Khalil, A. M. E., Eljamal, O., Jribi, S. & Matsunaga, N. 2016 Promoting nitrate reduction kinetics by nanoscale zero valent iron in water via copper salt addition. *Chem. Eng. J.* **287**, 367–380. http://dx.doi.org/10.1016/j.cej.2015.11.038.

Khani, A. & Mirzaei, M. 2008 Comparative study of nitrate removal from aqueous solution using powder activated carbon and carbon nanotubes. In *2nd International IUPAC Conference on Green Chemistry*, Russia, pp. 14–19.

Kim, H., Hong, H.-J., Jung, J., Kim, S.-H. & Yang, J.-W. 2010 Degradation of trichloroethylene (TCE) by nanoscale zero-valent iron (nZVI) immobilized in alginate bead. *J. Hazard. Mater.* **176**(1–3), 1038–1043. doi:10.1016/j.jhazmat.2009.11.145.

Kim, S. A., Kamala-Kannan, S., Lee, K.-J., Park, Y.-J., Shea, P. J., Lee, W.-H., Kim, H.-M. & Oh, B.-T. 2013 Removal of Pb(II) from aqueous solution by a zeolite–nanoscale zero-valent iron composite. *Chem. Eng. J.* **217**, 54–60. http://dx.doi.org/10.1016/j.cej.2012.11.097.

Li, G., Xu, Q., Jin, X., Li, R., Dharmarajan, R. & Chen, Z. 2018 enhanced adsorption and Fenton oxidation of 2, 4-dichlorophenol in aqueous solution using organobentonite supported nZVI. *Sep. Purif. Technol.* **197**, 401–406. https://doi.org/10.1016/j.seppur.2018.01.03.

Litter, M., Quici, N. & Meichtry, M. (Eds.). 2018 *Iron Nanomaterials for Water and Soil Treatment*. Jenny Stanford Publishing, New York, NY. https://doi.org/10.1201/b22501.

Liu, Y. & Wang, J. 2019 Reduction of nitrate by zero valent iron (ZVI)-based materials: a review. *Sci. Total Environ.* **671**, 388–403. https://doi.org/10.1016/j.scitotenv.2019.03.317.

Liu, A., Liu, J., Pan, B. & Zhang, W. 2014a Formation of lepidocrocite (γ-FeOOH) from oxidation of nanoscale zero-valent iron (nZVI) in oxygenated water. *RSC Adv.* **4**(101), 57377–57382. doi:10.1039/c4ra08988j.

Liu, Y., Li, S., Chen, Z., Megharaj, M. & Naidu, R. 2014b Influence of zero-valent iron nanoparticles on nitrate removal by paracoccus sp. *Chemosphere* **108**, 426–432. http://dx.doi.org/10.1016/j.chemosphere.2014.02.045.

Liyanage, C. E., Thabrew, M. I. & Kuruppuarachchi, D. S. P. 2000 Nitrate pollution in groundwater of Kalpitiya: an evaluation of the content of nitrates in the water and food items cultivated in the area. *J. Natn. Sci. Found. Sri Lanka* **28**(2), 101–112.

Lu, H.-J., Wang, J.-K., Ferguson, S., Wang, T., Bao, Y. & Hao, H. 2016 Mechanism, synthesis and modification of nano zerovalent iron in water treatment. *Nanoscale* **8**(19), 9962–9975. doi:10.1039/x0xx00000x.

Mikunthan, T., Vithanage, M., Pathmarajah, S., Arasalingam, S., Ariyaratne, R. & Manthrithilake, H. 2013 *Hydrogeochemical Characterization of Jaffna's Aquifer Systems in Sri Lanka*. International Water Management Institute (IWMI), Colombo, Sri Lanka, p. 69. doi:10.5337/2014.001.

Mohamed, F. D. & Lee, Y. W. 1988 Nitrate removal from water supplies using biological denitrification. *Water Pollut. Control Fed.* **60**(9), 1670–1674.

Mu, Y., Jia, F., Ai, Z. & Zhang, L. 2017 Iron oxide shell mediated environmental remediation properties of nano zero-valent iron. *Environ. Sci.: Nano* **4**(1), 27–45. doi:10.1039/C6EN00398B.

Mukherjee, R., Kumar, R., Sinha, A., Lama, Y. & Saha, A. K. 2016 A review on synthesis, characterization, and applications of nano zero valent iron (nZVI) for environmental remediation. *Crit. Rev. Environ. Sci. Technol.* **46**(5), 443–466. doi:10.1080/10643389.2015.1103832.

Nazli, E. 2008 *Characterization of the Adsorption Behaviour of Aqueous Cd(II) and Ni(II) Ions on Nanoparticles of Zero-Valent Iron*. Master's Thesis, School of Engineering and Science of İsmir Institute of Technology, Ismir, Turkey.

Nijamir, K. & Kaleel, M. I. M. 2017 The impact of agricultural practices on groundwater quality: a critical study based on Navithanveli division in Ampara district in Sri Lanka. *Int. J. Res. Granthaalayah* **5**(9), 36–43. https://doi.org/10.5281/zenodo.999195.

Peng, L., Liu, Y., Gao, S.-H., Chen, X., Xin, P., Dai, X. & Ni, B.-J. 2015 Evaluation on the nanoscale zero valent iron based microbial denitrification for nitrate removal from groundwater. *Sci. Rep.* **5**(1). doi:10.1038/srep12331.

Poursaberi, T., Konoz, E., Sarrafi, A. H. M., Hassanisadi, M. & Hajifathli, F. 2012 Application of nanoscale zero-valent iron in the remediation of DDT from contaminated water. *Chem. Sci. Trans.* **1**(3), 658–668. doi:10.7598/cst2012.246.

Ratnayake, S. Y., Ratnayake, A. K., Schild, D., Maczka, E., Jartych, E., Luetzenkirchen, J., Kosmulski, M. & Weerasooriya, R. 2017 Chemical reduction of nitrate by zerovalent iron nanoparticles adsorbed radiation-grafted copolymer matrix. *Nukleonika* **62**(4), 269–275. doi:10.1515/nuka-2017-0039.

Rocca, C. D., Belgiorno, V. & Meriç, S. 2007 Overview of *in-situ* applicable nitrate removal processes. *Desalination* **204**(1–3), 46–62. https://doi.org/10.1016/j.desal.2006.04.023.

Ryu, A., Jeong, S.-W., Jang, A. & Choi, H. 2011 Reduction of highly concentrated nitrate using nanoscale zero-valent iron: effects of aggregation and catalyst on reactivity. *Appl. Catal. B: Environ.* **105**(1–2), 128–135. doi:10.1016/j.apcatb.2011.04.002.

Salama, W., Aref, M. E. & Gaupp, R. 2015 Spectroscopic characterization of iron ores formed in different geological environments using FTIR, XPS, Mössbauer spectroscopy and thermoanalyses. *Spectrochim. Acta Part A: Molecular and Biomolecular Spectroscopy* **136**, 1816–1826. http://dx.doi.org/10.1016/j.saa.2014.10.090.

Samatya, S., Kabay, N., Yüksel, Ü., Arda, M. & Yüksel, M. 2006 Removal of nitrate from aqueous solution by nitrate selective ion exchange resins. *React. Funct. Polym.* **66**(11), 1206–1214. doi:10.1016/j.reactfunctpolym.2006.03.009.

Schoeman, J. 2009 Nitrate-nitrogen removal with small-scale reverse osmosis, electrodialysis and ion-exchange units in rural areas. *Water SA* **35**(5). doi:10.4314/wsa.v35i5.49198.

Schoeman, J. J. & Steyn, A. 2003 Nitrate removal with reverse osmosis in a rural area in South Africa. *Desalination* **155**(1), 15–26. https://doi.org/10.1016/S0011-9164(03)00235-2.

Water Practice & Technology Vol 15 No 4
doi: 10.2166/wpt.2020.086

Shukla, S. & Saxena, A. 2018 Global status of nitrate contamination in groundwater: its occurrence, health impacts, and mitigation measures. In: *Handbook of Environmental Materials Management* (Hussain, C. M., ed.). Springer International Publishing, Dordrecht, the Netherlands, pp. 1–21. https://doi.org/10.1007/978-3-319-58538-3_20-1.

Šimkovič, K., Derco, J. & Valičková, M. 2015 Removal of selected pesticides by nano zero-valent iron. *Acta Chimica Slovaca* **8**(2), 152–155. doi:10.1515/acs-2015-0026.

SLS 2013 *Specification for Potable Water – First Revision 614: 2013*. Sri Lanka Standards Institution, Colombo, Sri Lanka.

Sohrabi, M. R., Moghri, M., Masoumi, H. R. F., Amiri, S. & Moosavi, N. 2014 Optimization of Reactive Blue 21 removal by nanoscale zero-valent iron using response surface methodology. *Arabian J. Chem.* **9**(4), 518–525. http://dx.doi.org/10.1016/j.arabjc.2014.11.060.

Vaheesar, K. 2002 Nitrate and fluoride content in ground water in the Batticaloa district. *J. Sci., Eastern Univ. Sri Lanka* **2**(1), 9–15.

Wei, A., Ma, J., Chen, J., Zhang, Y., Song, J. & Yu, X. 2018 Enhanced nitrate removal and high selectivity towards dinitrogen for groundwater remediation using biochar-supported nano zero-valent iron. *Chem. Eng. J.* **353**, 595–605. https://doi.org/10.1016/j.cej.2018.07.127.

Wijeyaratne, W. M. D. N. & Subanky, S. 2017 Assessment of the efficacy of home remedial methods to improve drinking water quality in two major aquifer systems in Jaffna Peninsula, Sri Lanka. *Scientifica* **2017**, 1–6. https://doi.org/10.1155/2017/9478589.

World Health Organization 2017 *Guidelines for Drinking-Water Quality. Third Edition Incorporating the 1st Addendum*. World Health Organization, Geneva, Switzerland.

Yuvakkumar, R., Elango, V., Rajendran, V. & Kannan, N. 2011 Preparation and characterization of zero valent iron nanoparticles. *Dig. J. Nanomater. Biostructures* **6**(4), 1771–1776.

Zhang, Y., Douglas, G. B., Pu, L., Zhao, Q., Tang, Y., Xu, W., Luo, B., Hong, W., Cui, L. & Ye, Z. 2017 Zero-valent iron-facilitated reduction of nitrate: chemical kinetics and reaction pathways. *Sci. Total Environ.* **598**, 1140–1150. http://dx.doi.org/10.1016/j.scitotenv.2017.04.071.